



# On the temperatures developed in CFRP drilling using uncoated WC-Co tools Part II: Nanomechanical study of thermally aged CFRP composites



J.L. Merino-Pérez<sup>a,\*</sup>, A. Hodzic<sup>b</sup>, E. Merson<sup>c</sup>, S. Ayvar-Soberanis<sup>d</sup>

<sup>a</sup> Industrial Doctorate Centre in Machining Science, Department of Mechanical Engineering, The University of Sheffield, Sir Frederick Mappin Building, Mappin Street, Sheffield S1 3JD, UK

<sup>b</sup> Composite Systems Innovation Centre, Department of Mechanical Engineering, The University of Sheffield, Sir Frederick Mappin Building, Mappin Street, Sheffield S1 3JD, UK

<sup>c</sup> Sandvik Coromant, Sandvik AB, Advanced Manufacturing Park, Unit 8, Morse Way, Waverley, Sheffield S60 5BJ, UK

<sup>d</sup> Advanced Manufacturing Research Centre with Boeing, The University of Sheffield, Advanced Manufacturing Park, Wallis Way, Catcliffe, Rotherham S60 5TZ, UK

## ARTICLE INFO

### Article history:

Available online 20 December 2014

### Keywords:

Drilling of composites  
Thermosetting resin  
Nanoindentation  
Thermal ageing

## ABSTRACT

This study focused on the thermal degradation of the polymer phase of carbon fibre reinforced polymer (CFRP) composites through thickness by applying the nanoindentation technique. The results were compared for the elastic modulus ( $E$ ) and hardness ( $H$ ) of a non-aged sample and the samples aged at 200 °C and 350 °C during a short period of 60 s, in order to experimentally simulate the thermal conditions of drilling. Compared to the non-aged specimen, the results showed an increase of 16% in the elastic modulus and 12% in the hardness for the specimen aged at 200 °C. In contrast, the results for the specimen aged at 350 °C showed a variation of 0.8% and -3% in the elastic modulus and hardness respectively. These results contribute to a better understanding of the effect of the heat developed during the machining of composites on the properties of the resin phase in CFRP. Hereby we present the evidence of a post-curing effect at the temperatures close to the glass transition temperature ( $T_g$ ) in the drilling of CFRPs.

© 2014 The Authors. Published by Elsevier Ltd. This is an open access article under the CC BY license (<http://creativecommons.org/licenses/by/4.0/>).

## 1. Introduction

The dry machining of carbon fibre reinforced plastic (CFRP) composites showed to develop very high and localised temperatures, especially in drilling [1,2]. During the machining operations, the heat-affected zone (HAZ) is exposed to considerable amounts of heat during short periods that can produce an accelerated degradation of the polymer matrix and the reinforcement-matrix interphase. Early studies investigated the effects of accelerated ageing on the properties of bulk polymers and polymer matrix composites (PMC). Collings and Copley studied the accelerated ageing of CFRP systems and presented a model to predict the water absorption, which showed a good Fick-type correlation with the empirical results [3]. Ellis and Karasz studied the correlation between the water uptake and the depression of the glass transition temperature ( $T_g$ ) on DGEBA and TGDDM-based epoxy resins, and found that higher cross-linked systems were more sensible to this effect [4]. However, Valentin et al. conducted similar experiments on glass

fibre reinforced PA66 (thermoplastic matrix) composites and reported an increase of  $T_g$  with water absorption [5].

Later reports studied the effects of thermal ageing on the mechanical properties of PMC. Kim et al. investigated the heat-induced degradation of PEEK/epoxy/graphite composites during short ageing periods on the flexural properties of the composite using 4-point bend tests. They reported that the first order reactions, which occurred in the early stage degradation, accounted for the most part of the decay in the mechanical properties however had a little effect in the weight loss. However the second order reactions, which involved catalytic reaction of the reacting gases, had little impact on the mechanical properties but dominated weight loss [6]. Lévêque et al. utilised dynamic mechanical analysis (DMA) and monotonic creep tests to investigate the effect of thermal ageing on the properties of CFRP composites and reported dissimilar ageing mechanisms. If the ageing temperature was below  $T_g$ , consolidation (residual cross-linking) occurred, whereas above  $T_g$  chain rupture, oxidation and thermolysis was observed [7].

The work carried out by Oliver and Pharr allowed using nano mechanical techniques to study the properties of composites and their degradation [8]. Hodzic et al. first utilised the techniques of nano-scratch and nano-indentation to empirically measure the width of the fibre-matrix interphase [9,10] and studied the effects of water absorption on the properties of the polymer matrix and

\* Corresponding author. Tel.: +44 7592 962654.

E-mail addresses: [j.merino@sheffield.ac.uk](mailto:j.merino@sheffield.ac.uk) (J.L. Merino-Pérez), [a.hodzic@sheffield.ac.uk](mailto:a.hodzic@sheffield.ac.uk) (A. Hodzic), [eleanor.merson@sandvik.com](mailto:eleanor.merson@sandvik.com) (E. Merson), [s.ayvar@amrc.co.uk](mailto:s.ayvar@amrc.co.uk) (S. Ayvar-Soberanis).

the fibre–matrix interphase in polymer/glass composites [11,12]. Gregory and Spearing also applied the nano-indentation techniques to investigate the damage induced during the manufacturing process on the polymer phase in PMC by comparing the properties of the neat resin and the matrix of *in situ* manufactured composites [13]. A modified micro indentation technique using a nano indenter apparatus was successfully applied by Haerberle et al. to study the fibre/matrix interfacial shear strength of composites subjected to hygrothermal ageing [14].

The thermal and the hygrothermal degradation of the matrix and the reinforcement–matrix interphase in PMC was carried out using a number of techniques. Odegard and Bandyopadhyay reviewed and discussed the effects of physical ageing (sub- $T_g$  exposure) on the thermo mechanical properties of epoxy resins and epoxy-based composites concluding that, after long ageing periods, the reduction of free volume and the changes in the molecular structure (residual cross-linking) affected the bulk properties of the polymer such in a way that significantly changed the response of the material [15].

In more recent studies, Li et al. utilised a single fibre fragmentation test to investigate the influence of the carbon fibre (CF) surface characteristics on the interfacial bonding of aged carbon/epoxy composites, and reported that the silicon content on the CFs had a significant impact on the fibre–matrix bonding properties [16]. Further work evaluated also the interfacial properties of aged carbon/epoxy composites by studying the interlaminar shear strength (ILSS) and the interfacial fracture energy. They concluded that the micro and macro interfacial hygrothermal resistance had a strong correlation, whereas the interfacial fracture energy was more convenient to assess the interfacial bonding in water ageing [17]. Dokukin and Sokolov investigated the elastic modulus and hardness of a number of soft polymers using the small depth nano-indentation, reported and discussed an observed *skin effect*. The authors concluded that this effect appeared when using very sharp indenters ( $\sim 22$  nm tip radius) due to a nonlinearity stress–strain relation and if the tip-surface adhesion is not taken into account [18]. Cakmak et al. performed a surface characterisation and studied the surface adhesion of reactor-thermoplastic-polyolefin-copolymers (R-TPO) for automotive applications by the nano-indentation techniques in the open loop (OL), displacement control (DC) and load control (LC) modes. The authors found that the adhesion force decreased with both the increasing elastic modulus and hardness [19]. Lorenzo et al. studied the properties of nanocomposites formed by recovered polycarbonate (PC) and organic modified nanoclays and compared their mechanical properties with those of virgin PC by depth sensing indentation (DSI) techniques. They reported that greater nanoclay contents not always increased the mechanical properties and explained this behaviour by the reinforcement effect of the nanofillers being counteracted by the thermal and mechanical degradation of the recovered PC during its recycling process [20].

The work presented in this investigation applied the nano-indentation technique to study the mechanical properties (elastic modulus and hardness) of the polymer phase of CFRP composites aged at temperatures in the vicinity of  $T_g$  during a short ageing period, in order to detect the influence of thermal energy during the composites machining.

## 2. Materials and methods

### 2.1. Composite system

The CFRP specimens utilised in this study were manufactured at the Composite Centre of the Advanced Manufacturing Research Centre with Boeing, The University of Sheffield, and the composite

system used in this study was MTM44-1 CF0300. MTM44-1 resin is a toughened phenol–formaldehyde (PF)-based aerospace grade resin having an onset glass transition temperature ( $T_g$ ) of approximately 190 °C, whereas CF0300 is a 2/2-twill carbon fabric, 3K high strength (HS) carbon fibre reinforcement.

Initially, 750 × 500 mm plate was manufactured using the vacuum bag moulding method, by laying up 11 prepreg plies to approximate thickness of 2 mm. These prepreg plies, supplied by Cytec Engineered Materials, consisted of woven carbon fibre (CF) fabric and epoxy resin having 55% fibre volume fraction ( $V_f$ ). Following the lay-up operation, the composite plate was cured and post-cured in an autoclave according to the specifications provided by the supplier to develop its full mechanical properties and the maximum  $T_g$ . Before the ageing process, the plate was cut down to different sizes to produce test coupons for different studies, following the standard *EN ISO 2818:1996 Plastics – Preparation of test specimens by machining*. The size of the specimens used in this study was 30 × 20 × 2 mm.

### 2.2. Thermal analysis

The decomposition of MTM44-1 resin was studied with differential scanning calorimetry (DSC) and thermogravimetric (TGA) analyses. MTM44-1 solid resin, casted and supplied by Cytec Engineered Materials, was ground to powder size using a *Retsch Mixer Mill Cryo-Mill* milling machine. This machine had a drum where the solid resin was introduced together with a steel ball, and used liquid nitrogen to cool the system down to –190 °C, thus embrittling the resin and facilitating its fracture. A pre-cooling cycle of 3 min was set to cool down the system, followed by a 15 min grinding cycle during which the drum was shaken at 25 Hz. The powder resin obtained was dried inside an oven at 50 °C during 24 h and then stored inside a desiccator (diphosphorus pentoxide,  $P_2O_5$ ).

The thermal analyses were performed using a *PerkinElmer Simultaneous Thermal Analyzer STA8000*, by performing DSC and TGA analyses at once. 40 mg of powder MTM44-1 resin was analysed by performing a temperature sweep from room temperature up to 400 °C. The results obtained in this way,  $\Delta T$  and weight loss (%) vs. temperature, were then processed using *PerkinElmer PYRIS* software.

### 2.3. Ageing

**Table 1** shows the ageing conditions considered in this study. The test specimens were aged using a *Carbolite 1806/SIRIUS/LEV3* furnace, fitted with a thermocouple for a better temperature control. The samples were placed in the middle of the chamber close to the thermocouple, which allowed the ageing temperatures to be measured with high accuracy. A steel mail fixture helped to introduce and withdraw the specimens in the chamber rapidly, thus reducing the temperature fluctuation. After the ageing process, the samples were cooled down to room temperature in still air.

### 2.4. Specimen preparation for the nano-indentation technique

The test specimens were sliced following *EN ISO 2818:1996* standard, in order to obtain 15 × 20 × 2 mm specimens. The

**Table 1**  
Ageing conditions. Condition 1 represents the non-aged specimen.

Condition	Ageing temperature (°C)	Ageing time (s)
1	–	–
2	200	60
3	350	–

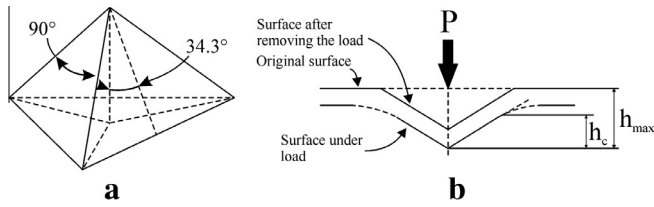


Fig. 1. Illustrative descriptions of (a) the geometry of a cube-corner tip and (b) the sketch of an indentation showing the depths used in the analyses.

specimens were cold mounted in epoxy resin to avoid any further thermal damage and the new exposed surfaces were polished using an *EcoMet 250* grinding-polishing machine manufactured by Buehler. The grinding was conducted using P400, P800 and P1200 grit size silicon carbide discs, whereas the polishing utilised 6  $\mu\text{m}$ , 3  $\mu\text{m}$ , 1  $\mu\text{m}$  and 0.25  $\mu\text{m}$  diamond suspensions. Prior to the indentations, the samples were conditioned and dried inside a desiccator using  $\text{P}_2\text{O}_5$ .

### 2.5. The nano-indentation technique

The device utilised in this work was a hybrid system composed of *Dimension 3100* scanning probe microscope (SPM) manufactured by Veeco Digital Instruments and *TS-70 TriboScope* nano-mechanical test system manufactured by Hystrion. The SPM was fitted with a high magnification monochrome optical camera for a precise placement of the probe on the sample, and operated in atomic force microscope (AFM) contact mode. The specimens were accurately positioned in X, Y and Z axes using a motorised table and the optical imaging system. The indenter mounted on the test system was a Cube-Corner diamond tip, a three-sided pyramidal indenter with the faces arranged in a shape like the corner of a cube, with the geometry described in Fig. 1. The sharper geometry of the cube-corner tip compared to that of the standard Berkovich tip allowed the plastic deformation produced by the indentations to be contained inside a smaller volume.

In order to study the mechanical properties of the polymer phase through-thickness, three resin-rich areas were selected from

the edge to approximately 1/2 the specimen thickness. Fig. 2 shows the areas of interest considered on each test specimen, obtained with *Nikon Eclipse LV150* optical microscope attached to a computer.

A set of 25 indentations were performed on each selected area in  $5 \times 5$  array, using 4  $\mu\text{m}$  spacing between indents. Therefore, each CFRP specimen was indented 75 times. Each indentation was programmed to apply a force of 50  $\mu\text{N}$  following a trapezoid sequence (5 s load, 5 s dwell and 5 s unload). As a result of applying a constant force, the indentation depth varied with the hardness of the material. The load–displacement curves were then analysed as described by Oliver and Pharr [8]. The hardness of the material is then calculated taking into account the load applied, the contact depth (Fig. 1(b)) and the shape of the tip, as shown in the equation below:

$$H = \frac{P_{max}}{A_p} \quad (1)$$

where  $P_{max}$  corresponds to the load applied and  $A_p$  is the projected contact area, which depends on the type of indenter used and on the contact depth following a polynomial relationship. When performing shallow indents, the equation can be reduced to:

$$A_p = C_0 \cdot h_c^2 \quad (2)$$

where the value of  $C_0$  corresponding to an ideal cube-corner probe is 2.598. However, this value needs to be recalculated as the tip wears out. The reduced modulus ( $E_r$ ) can be obtained from the unloading curve (Fig. 3) obtained for each indentation and is calculated using the following equation:

$$E_r = \frac{S\sqrt{\pi}}{2\sqrt{A_p}} \quad (3)$$

$A_p$  is the projected contact area and  $S$  is the stiffness of the unloading curve. The slope of the initial portion of the unloading curve can be obtained from the equation:

$$S = \frac{dP}{dh} \quad (4)$$

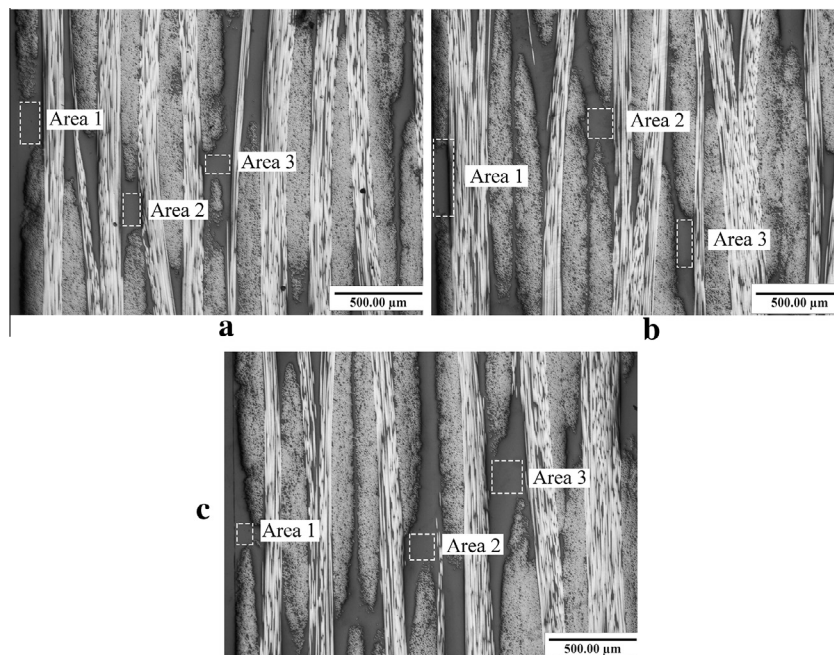
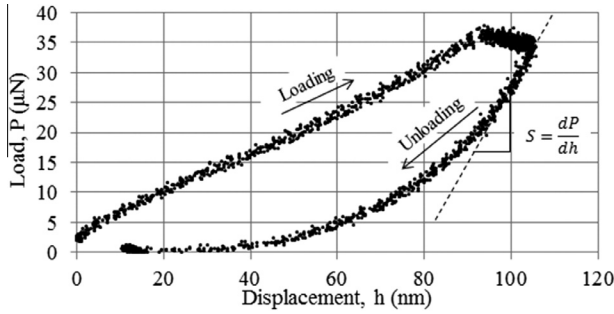


Fig. 2. Indented areas on (a) the non-aged specimen and the specimens aged at (b) 200 °C and (c) 350 °C.



**Fig. 3.** Example of load vs. displacement curve obtained after the indentation of MTM44-1 polymer used in this study.

where  $P$  is the measured indentation load and  $h$  the measured penetration depth. Then, the elastic modulus of the indented material can be calculated with the expression below, which relates the elastic properties of the diamond tip, the material and the reduced elastic modulus:

$$E_r = \left( \frac{1 - \nu_{indenter}^2}{E_{indenter}} + \frac{1 - \nu_{material}^2}{E_{material}} \right)^{-1} \quad (5)$$

where  $\nu$  is the Poisson's ratio and  $E$  is the elastic modulus. For a diamond tip, the typical values of elastic modulus and Poisson's ratio are 1140 GPa and 0.07 respectively. The modulus of elasticity of the tested material for each indent was therefore calculated with its Poisson's ratio, which can be obtained from the literature.

### 3. Results and discussion

#### 3.1. Through-thickness nano-mechanical properties

Table 2 shows the values of elastic modulus ( $E$ ) and hardness ( $H$ ) through the samples thickness obtained from the nano-indentations. The values of elastic modulus were calculated applying the reduced elastic modulus ( $E_r$ ) obtained from the indentations into Eq. (5).

The values of elastic modulus and hardness measured in areas at different thickness levels revealed consistent results through the samples. Therefore, the ageing period (60 s) applied to the samples aged at 200 °C and 350 °C were sufficient to age the samples uniformly through the whole thickness.

#### 3.2. Mechanical properties vs. ageing temperature

Fig. 4 illustrates three nano-indentations curves that are representative of those obtained in testing samples of the selected CFRP composite aged at the three different conditions considered in this study.

The results showed that although the indentation load was set to 50 µN, the actual measured load was close to 38 µN. The reason for obtaining a lower load value is that the system compensated the spring force, which was around 12 µN. The maximum indentation width can be measured directly using the AFM imaging system or calculated manually. Assuming that the shape of the cube corner

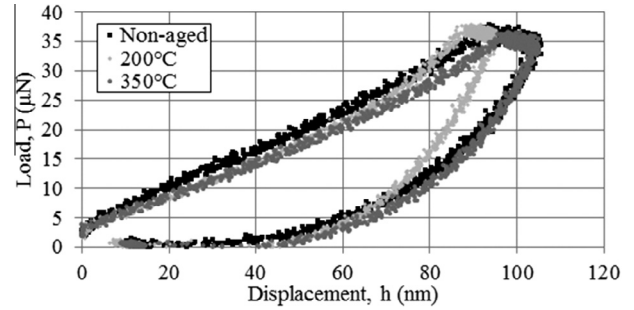


**Fig. 4.** Loading vs. displacement curves obtained in testing resin phases of MTM44-1 CF0300 samples aged at different conditions.

tip is perfect (Fig. 1) and taking into account the maximum penetration depth ( $h_{max}$ ), the calculated maximum indentation width ranged between 325 and 360 nm.

Fig. 5 compares the values of elastic modulus and hardness obtained from the indentations performed on samples aged at three different conditions (Table 1).

The results showed similar trends for the elastic modulus and hardness. Taking the values corresponding to the non-aged sample as the reference, the sample aged at 200 °C yielded an increase of 16% and 12% in the elastic modulus and the hardness respectively. However, the sample aged at 350 °C showed an increase of 0.8% in the elastic modulus and a decrease of 3% in the hardness. This behaviour can be explained by a post-curing effect at ageing temperatures close to the  $T_g$ , and a post-curing effect followed by further damage at temperatures above the  $T_g$  of the resin [7].

At ageing temperatures up to  $T_g$ , physical ageing mechanisms dominated the ageing process. It was reported that the physical ageing involved residual cross-linking and molecular rearrangement [6]. During this process, an increase in cross-linking density resulted in the increased elastic modulus [21–23], thus explaining the results obtained in this study.

At ageing temperatures above  $T_g$  of the polymer, chemical ageing mechanisms occurred. Chemical ageing involved chain rupture, oxidation [6] and, at high temperatures, also catalytic reaction of gases and pyrolyzation [7]. Fig. 6 illustrates the results of the thermal analyses of MTM44-1 resin.

The DSC curve showed two endothermic peaks, which matched two decomposition stages, as showed by the TGA curve. The first endothermic reaction appeared at the onset of 210 °C and corresponded to an early degradation stage (–0.2%/min), whereas the second endothermic reaction occurred at the onset of 350 °C and corresponded to a severe decomposition phase (–15.5%/min). The highest ageing temperature used in this study, 350 °C, was above the early decomposition stage and corresponded to an intermediate decomposition rate (–1.1%/min). Hence, degradation mechanisms that produce weight loss occur at this ageing temperature.

Literature reported that the degradation mechanisms taking place at later decomposition stages (oxidation, catalytic reaction of \*\*gases) caused the weight loss. Although these were reported to have a little effect on the mechanical properties, they were preceded by other degradation mechanisms (polymer chain rupture) that did have a significant impact on the mechanical properties

**Table 2**

Values of elastic modulus ( $E$ ) and hardness ( $H$ ) corresponding to areas 1 (edge of the sample), 2 (approx.1/4 thickness) and 3 (approx. 1/2 thickness) of CFRP samples aged at different conditions (Table 1). Each value is the average of 25 indentations.

Ageing condition	Area 1		Area 2		Area 3	
	Elastic modulus, $E$ (GPa)	Hardness, $H$ (GPa)	Elastic modulus, $E$ (GPa)	Hardness, $H$ (GPa)	Elastic modulus, $E$ (GPa)	Hardness, $H$ (GPa)
1	3.76	0.42	3.34	0.38	3.47	0.40
2	4.01	0.43	4.10	0.46	4.14	0.44
3	3.43	0.38	3.59	0.39	3.66	0.38

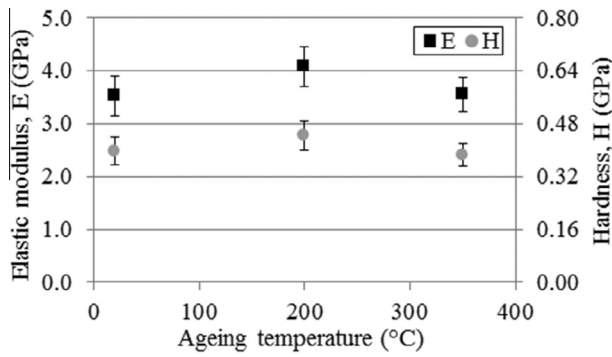


Fig. 5. Values of elastic modulus and hardness vs. ageing temperature ( $\pm$ SD). Each point represents the average of 75 indentations per sample (25 indentations on each selected area, three selected areas per sample).

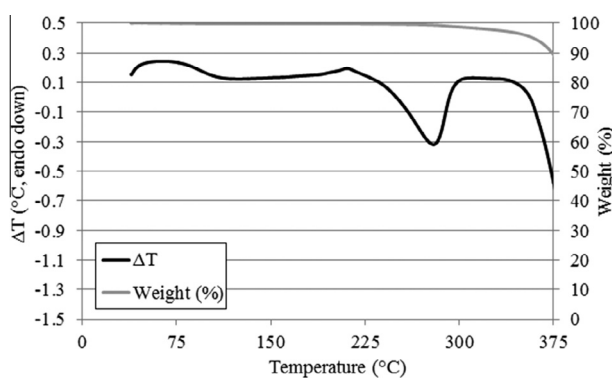


Fig. 6. Differential scanning calorimetry (DSC) and thermogravimetric (TGA) analyses of MTM44-1 resin.

of the polymer [6], thus explaining the values of the mechanical properties obtained in the sample aged at 350 °C. These results are in good agreement with the results obtained in our study about the effect of heat during short ageing periods on the tensile strength and impact energy absorption of CFRP composites [24].

#### 4. Conclusions

The work presented investigated the mechanical properties of the resin phase of CFRP composites aged at different temperatures during short periods. Based on the analysis of the results obtained in this investigation, the following conclusions can be summarised:

- A short ageing period (60 s) was sufficient to age the selected samples uniformly through the thickness (2 mm).
- Ageing temperatures up to  $T_g$  increased the cross-linking density due to a heat-induced residual cross-linking, therefore increasing the elastic modulus (+16%) and the hardness (+12%) of the resin phase, compared to the non-aged specimen.
- Ageing temperatures above the  $T_g$  of the resin showed a significant decrease of the elastic modulus (−13%) and the hardness (−14%) compared to the samples aged at temperatures close to  $T_g$ .
- After the post cross-linking effect, further degradation mechanisms occurred that accounted for the reduction in the mechanical properties (polymer chain rupture) and weight loss (oxidation, pyrolysis).
- The variation of the properties of the resin phase had an impact on the ability of the resin to transfer the load to the reinforcement, thus affecting the macro mechanical properties

(e.g. tensile strength) of the composite. This will help to understand the variation of the mechanical properties of the heat-affected zone during the machining operation.

#### Acknowledgements

This work was co-funded through the EPSRC Industrial Doctorate Centre in Machining Science (EP/I01800X/1) and by Sandvik Coromant.

#### References

- [1] Merino-Pérez JL, Merson E, Ayvar-Soberanis S, Hodzic A. The applicability of Taylor's model to the drilling of CFRP using uncoated WC-Co tools: the influence of cutting speed on tool wear. *Int J Mach Mach Mater* 2014;16(2):95–112.
- [2] Merino-Pérez JL, Royer R, Ayvar-Soberanis S, Merson E, Hodzic A. On the maximum temperatures developed in CFRP drilling using uncoated WC-Co tools – Part I: The influence of the workpiece constituents and cutting speed on heat dissipation, *Compos Struct*, 2014, <http://dx.doi.org/10.1016/j.compstruct.2014.12.033>.
- [3] Collings TA, Copley SM. On the accelerated ageing of CFRP. *Composites* 1983;14(3):180–8.
- [4] Ellis TS, Karasz FE. Interaction of epoxy resins with water: the depression of glass transition temperature. *Polymer* 1984;25(5):664–9.
- [5] Valentin D, Paray F, Guetta B. The hygrothermal behaviour of glass fibre reinforced Pa66 composites: a study of the effect of water absorption on their mechanical properties. *J Mater Sci* 1987;22(1):46–56.
- [6] Kim J, Lee WI, Tsai SW. Modeling of mechanical property degradation by short-term aging at high temperatures. *Compos B Eng* 2002;33(7):531–43.
- [7] Lévêque D, Schieffer A, Mavel A, Maire JF. Analysis of how thermal aging affects the long-term mechanical behavior and strength of polymer-matrix composites. *Compos Sci Technol* 2005;65(3–4):395–401.
- [8] Oliver WC, Pharr GM. Improved technique for determining hardness and elastic modulus using load and displacement sensing indentation experiments. *J Mater Res* 1992;7(6):1564–80.
- [9] Hodzic A, Kim JK, Stachurski ZH. Nano-scratch technique as a novel method for measurement of an interphase width. *J Mater Sci Lett* 2000;19(18):1665–7.
- [10] Hodzic A, Stachurski ZH, Kim JK. Nano-indentation of polymer-glass interfaces. Part I. Experimental and mechanical analysis. *Polymer* 2000;41(18):6895–905.
- [11] Hodzic A, Kim JK, Stachurski ZH. Nano-indentation and nano-scratch of polymer/glass interfaces. II: Model of interphases in water aged composite materials. *Polymer* 2001;42(13):5701–10.
- [12] Hodzic A, Kim JK, Lowe AE, Stachurski ZH. The effects of water aging on the interphase region and interlaminar fracture toughness in polymer-glass composites. *Compos Sci Technol* 2004;64(13–14):2185–95.
- [13] Gregory JR, Spearing SM. Nanoindentation of neat and in situ polymers in polymer-matrix composites. *Compos Sci Technol* 2005;65(3–4):595–607.
- [14] Haerberle DC, Lesko JJ, Case SW, Riffle JS, Verghese KE. The use of a modified microindentation technique to evaluate enviro-mechanical changes in composite interphase properties. *J Adhes Sci Technol* 2007;21(1):35–50.
- [15] Odegard GM, Bandyopadhyay A. Physical aging of epoxy polymers and their composites. *J Polym Sci, Part B: Polym Phys* 2011;49(24):1695–716.
- [16] Li M, Liu H, Gu Y, Li Y, Zhang Z. Effects of carbon fiber surface characteristics on interfacial bonding of epoxy resin composite subjected to hygrothermal treatments. *Appl Surf Sci* 2014;288:666–72.
- [17] Gu Y, Liu H, Li M, Li Y, Zhang Z. Macro and micro-interfacial properties of carbon fiber reinforced epoxy resin composite under hygrothermal treatments. *J Reinf Plast Compos* 2014;33(4):369–79.
- [18] Dokukin ME, Sokolov I. On the measurements of rigidity modulus of soft materials in nanoindentation experiments at small depth. *Macromolecules* 2012;45(10):4277–88.
- [19] Cakmak UD, Schöberl T, Major Z. Nanoindentation of polymers. *Meccanica* 2012;47(3):707–18.
- [20] Lorenzo V, De La Orden MU, Muñoz C, Serrano C, Martínez Urreaga J. Mechanical characterisation of virgin and recovered polycarbonate based nanocomposites by means of depth sensing indentation measurements. *Eur Polym J* 2014;55(1):1–8.
- [21] Lesser AJ, Crawford E. The role of network architecture on the glass transition temperature of epoxy resins. *J Appl Polym Sci* 1997;66(2):387–95.
- [22] Crawford E, Lesser AJ. The effect of network architecture on the thermal and mechanical behavior of epoxy resins. *J Polym Sci, Part B: Polym Phys* 1998;36(8):1371–82.
- [23] Bandyopadhyay A, Odegard GM. Molecular modeling of crosslink distribution in epoxy polymers. *Modell Simul Mater Sci Eng* 2012;20(4).
- [24] Merino-Pérez JL, Ayvar-Soberanis S, Merson E, Hodzic A. The influence of heat during short ageing periods on the mechanical properties of CFRP composites. In: Proceedings of the 16th European conference on composite materials (ECCM16), Seville, 22–26 June 2014, p. 8, <http://dx.doi.org/10.13140/2.1.2416.7368>.